frontiers | Frontiers in Energy Research

TYPE Original Research
PUBLISHED 27 September 2022
DOI 10.3389/fenrg.2022.1006421

OPEN ACCESS

EDITED BY
Sukru Merey,
Batman University, Turkey

REVIEWED BY
Lin Chen,
Institute of Engineering Thermophysics (CAS), China
Aliakbar Hassanpouryouzband,
University of Edinburgh,
United Kingdom

*CORRESPONDENCE
Zhibin Yang,
zfugui@mail.cgs.gov.cn

SPECIALTY SECTION
This article was submitted to Advanced Clean Fuel Technologies, a section of the journal Frontiers in Energy Research

RECEIVED 29 July 2022
ACCEPTED 08 September 2022
PUBLISHED 27 September 2022

CITATION
Zhang F, Yang Z, Zhou Y, Zhang S and Yu L (2022), Accumulation mechanism of natural gas hydrate in the Qilian Mountain permafrost, Qinghai, China. *Front. Energy Res.* 10:1006421. doi: 10.3389/fenrg.2022.1006421

Accumulation mechanism of natural gas hydrate in the Qilian Mountain permafrost, Qinghai, China

Fugui Zhang[1], Zhibin Yang[1]*, Yalong Zhou[1], Shunyao Zhang[1] and Linsong Yu[2]

[1]Institute of Geophysical and Geochemical Exploration, Chinese Academy of Geological Sciences, Langfang, China, [2]Shandong Institute of Geophysical and Geochemical Exploration, Jinan, China

Qilian Mountain is the only permafrost area in China where natural gas hydrates have been obtained through scientific drilling. Many studies have been performed on natural gas hydrates in permafrost regions from the perspectives of sedimentology and petroleum geochemistry, especially on reservoir forming conditions and exploration methods. However, there are still more divergences in its evolutionary process, time, and accumulation mechanism. In this study, a total of 500 core samples were collected in the gas hydrate drilling wells DK-8, DK13-11, and DK12-13 in the Qilian Mountain permafrost. Gas components, carbon isotopes of methane, total organic carbon (TOC), chloroform bitumen "A," concentrations of kerogen element, and vitrinite reflectance (*Ro*) are analyzed. The results show that the hydrocarbon source rocks in the Middle Jurassic Muli formation and the Upper Triassic Galedesi formation are good source rocks, with good total organic carbon content and chloroform bitumen "A." The rocks of Muli formation are at the mature stage of organic matters, and the organic matter types are mainly II_1 and II_2 and the peak of generating crude oil with immense petroleum-associated gas. Also, the rocks of the Galedesi formation are in a highly mature stage, producing more gas and offering efficient gas for the natural gas hydrate, and the organic matter types are mainly III and II_1. Laboratory experiments and numerical analysis indicate that the formation of natural gas hydrates in the Qilian Mountain has experienced three phases: gas migration and aggregation in the Late Jurassic to Early Cretaceous, overall uplift in the Middle and Late Miocene to Pliocene, and free gas to natural gas hydrate deposits in the Quaternary. The experimental results show that gas sources, permafrost thickness, and structural conditions played a key role in controlling the occurrence and distribution of gas hydrates.

KEYWORDS

natural gas hydrate, source rock, accumulation mechanism, gas migration, Qilian Mountain permafrost

1 Introduction

Natural gas hydrate (NGH) is a kind of crystalline solid substance formed by water and gas molecules (mainly methane) at low temperature and high pressure, widely distributed in submarine sediments, permafrost areas, and some deep lake deposits (Kvenvolden, 1993; Collett, 1994; Makogon et al., 2007; Collett et al., 2011). With the increasing need for energy and stricter requirements for the environment worldwide, every government attaches great importance to development and utilization of NGH (Boswell et al., 2012; Lee and Collett, 2013; Konno et al., 2017; Li et al., 2018; Collett et al., 2019). NGH is also the most important carbon pool in the shallow crust and is extremely sensitive to temperature and pressure changes (Farahani et al., 2021a). Although quantification of hydrates in permafrost sediments has always been a major challenge in the study of the climate-driven evolution of gas hydrate-bearing permafrost sediments due to almost identical acoustic properties of hydrates and ice (Farahani et al., 2021b), the fact that NGH could have a synergistic relationship with climate change processes has been supported by many studies (Hassanpouryouzband et al., 2020; Thomas et al., 2020). NGH and past climate events have been linked in some articles, and researchers have investigated the possible synergies, especially for the "snowball Earth," "mass extinction," and "Paleocene–Eocene thermal maximum hyperthermal event" (Katz et al., 1999; Hesselbo et al., 2000; Kennedy et al., 2008; Shakhova et al., 2010), which play an important role in the process of global climate change. In 2017, the production test of NGH in the Shenhu area in the South China Sea achieved stable gas production for 60 days, with the cumulative gas production exceeding 309,000 cubic meters, making a historic breakthrough in the trial production of NGH (Li et al., 2018; Liang, et al., 2019; Ye, et al., 2020). The potential of NGH resources remains huge not only in the sea area but also in permafrost regions in China (Zhu et al., 2010, 2011; Lu et al., 2011). Particularly, in 2008, the China Geological Survey (CGS) obtained experimental samples of hydrates in the Qilian Mountains for the first time, which was the first time that hydrates were found in the global mid-latitude permafrost (Zhu et al., 2010). A major breakthrough has been made in NGH exploration in the permafrost regions; consequently, a series of achievements have been made in the past 10 years, such as exploration methods and techniques of reconnaissance and trial mining. At the same time, a new understanding has been formed in the field of basic research (Lu et al., 2013; Wang et al., 2015, 2014; Sun et al., 2014; Fang et al., 2017; Lin et al., 2018; Zhao et al., 2018; Wang et al., 2019; Zhang et al., 2019). The aggregation process of NGH embraces gas generation, migration, accumulation, and storage. More emphasis was always placed on the study of the genesis of gas (Huang et al., 2016; Tan et al., 2017; Lu et al., 2020; Ning et al., 2020), and people have got a further understanding of the process of gas migration and accumulation in recent years (Wang et al., 2014; Lu et al., 2015). However, there is still no consensus on the gas source and on the accumulation process of NGH in the permafrost, so studies on gas migration and trap are still not matured (Lu et al., 2011, 2013; Dai et al., 2014). Moreover, the complexity of tectonics and lithological characters in the research region leads to difficulty in horizontal comparison of NGH, even though the boreholes are less than 100 m apart, so the research on the geochemical accumulation mechanism of NGH is not in-depth enough and remains in the speculation stage (Zhai et al., 2014; Li et al., 2017; Zhang et al., 2020). Based on the geochemical research studies in recent years, this study puts forward the NGH accumulation mechanism in the permafrost region, ranging from the evaluation of source rock, the gas resource and genesis, and the vertical migration mechanism of hydrocarbon and hydrocarbon generation history.

2 Geological settings

The Southern Qilian Basin is located in the northeastern part of the Qinghai–Tibetan Plateau in China. Its tectonic units are usually divided into Shule depression, Muli depression, Xiariha depression, Halahu depression, and Tianjun depression (Figure 1A). "Scientific Drilling Project of Gas Hydrate" is located in the Muri coalfield, Tianjun County, Qinghai province of China, where eleven wells were implemented by the China Geological Survey and Shenhua Qinghai Energy Co., Ltd., as shown in Figure 1B. The study region was influenced by the first act of the Yanshan movement in the Early Jurassic and underwent transformation from a compressed environment in Triassic to an extensional environment, and then this area, settled under the extensional tectonic stress, deposits a set of coal-bearing clastic rocks with fluvial-lacustrine, swamp facies in the Jurassic period. The second episode of the Yanshan movement during the Late Jurassic epoch to the Paleocene epoch resulted in regional angular unconformity between the pre-Cretaceous strata and Cretaceous strata. Since the Cenozoic era, the Tibetan Plateau has been experiencing crustal shortening and deformation at the northeastern margin, as well as the strike-slipping of the Altun fault at the western margin, which forged the NWW-trending and NNW-trending thrust faults in Qilian Mountain (Figure 1B) (Wen et al., 2011). The Juhugeng mining area remains on the syncline axis around 50–70 degrees north by west with complex anticline and syncline structures, consisting of one anticline and two syncline structures (Fu and Zhou, 2000). The exposed strata in the mining area mainly include the Middle Jurassic Jiangcang formation (J_2j) and the Muli formation (J_2m), each containing multiple coal-bearing strata (Niu et al., 2015) (Figure 1B), serving as the key to exploration of NGH. The Upper Triassic Galedesi formation (T_1g), with dark mudstone, black mudstone, oil shale, and thin coal seam as its main lithological characteristics, is widely exposed in the north and south of the Juhugeng mining area and at its anticlinal axis part, which

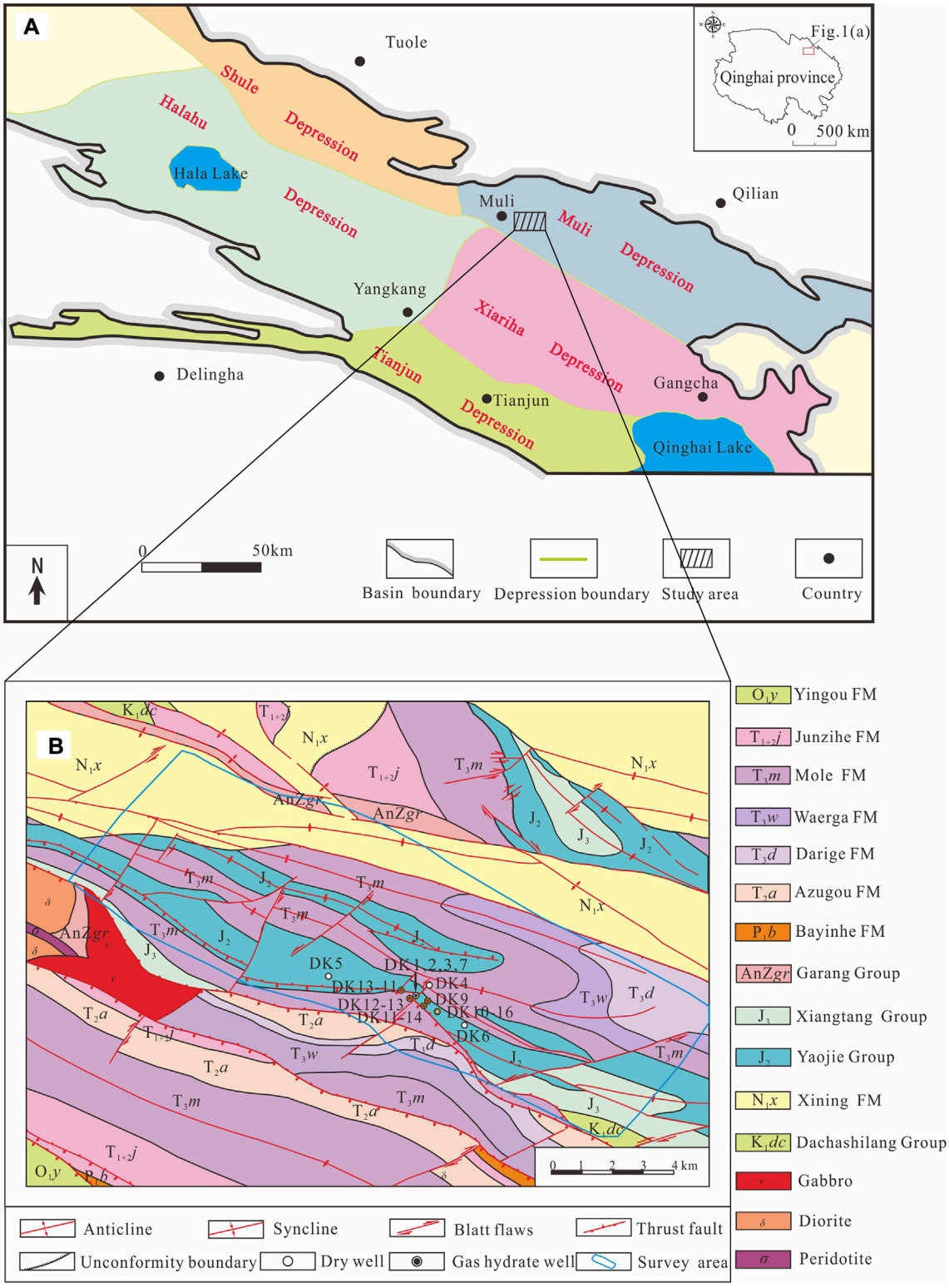

FIGURE 1
(A) Schematic map of the Southern Qilian Basin showing the distribution of tectonic units and the location of the Scientific Drilling Project of gas hydrate (modified from Fu and Zhou, 2000). **(B)** Geological map for the study area in the Qilian Mountain permafrost (modified from Wang et al., 2014).

TABLE 1 Hydrocarbon source rock evaluation in Qilian Mountain permafrost.

Series	Group	TOC	Chloroform bitumen A	Kerogen type	*Ro*	S_1+S_2	(Tmax/°C)
Middle Jurassic	Muli formation	>1% samples account for 83.33%	0.0136–0.1595%, average 0.0916%, and >0.05% account for 86.33%	II_2, II_1	0.68–1.27%	0.21–6.18 mg/g, average index: 3.40 mg/g	452–461°C, average temperature: 456°C
Upper Triassic	Galedesi formation	>1% samples account for 88.75%	0.0017–0.0526%, average 0.0284%, and <0.05% account for 94.12%	III, II_1	1.04–1.81%	0.05–1.39 mg/g, average index: 0.58 mg/g	465–537°C, average temperature: 472°C

Note: S_1, free hydrocarbons (mg/g) and S_2, pyrolytic hydrocarbons (mg/g).

stratigraphically shows disconformity with the overlying Jurassic. This formation is the main source rock and serves as a potential oil and gas area depending on its relatively well-developed reservoir (Fu and Zhou, 2000).

3 Materials and methods

Core samples were collected from three wells in the Muli permafrost of the Qilian Mountain, namely, well DK-8, well DK13-11, and well DK12-13. The depth of well DK-8 remains was 401.5 m, and 400 core samples were collected at a burial depth of 104.6–401.5 m, with each sampling site 2 m apart and 1 m apart in the NGH discovery layer or indeterminate layer. A part of the core samples was placed in a bottle pre-filled with 200 ml of saturated salt water so that the liquid level of the saturated salt water increased to 400 ml. The main component of table salt is NaCl, which has the properties of ionic crystal and light hydrocarbon adsorption. Saturated salt water was added to exhaust the air to form a vacuum inside, and the physical adsorption of the hydrocarbon can be completely released. Then, the screws and cap of the bottle were tightened and put upside down in the room to maximize the storage of headspace gas in the samples and analyzed the headspace gas. The other core samples, lined with cellophane, were packaged into belt transects and sent directly to the laboratory for analyzing methane stable carbon isotopes. Then, 40 core samples were selected from well DK12-13 for source rock analysis, including six samples from the Jurassic Muli formation and 34 samples from the Upper Triassic Galedesi formation. The main test indexes were total organic carbon (TOC), chloroform bitumen "A," concentrations of kerogen element, and vitrinite reflectance (*Ro*).

The headspace gas samples from the cores and the methane stable carbon isotope were analyzed at the Sinopec Training & Testing Center in Hefei. After being sent to the laboratory, the headspace sample was shaken well and allowed to rest for some time, and then a vacuum syringe with a metal needle was used to transfer the gas from the headspace of the vial into the gas chromatograph. According to the standards of "Method for Samples Determination of Petroleum Geochemical Exploration" (GB/T29173-2012), total concentrations of methane, ethane, propane, and butane were measured by a gas chromatograph-hydrogen flame ionization detector (GC-FID, universal natural gas analyzer 8,890, area repeatability, 0.5% RSD, Agilent Technologies, United States), with μL/L as the unit (the gas component volume (L) per liter of head space volume), and all detection limits of test indexes remain 0.02μ L/L. The methane stable carbon isotope measurement refers to the process that converted the prepared hydrocarbons into pure CO_2 gas, was measured by gas chromatography-mass spectrometry (GC-MS, stable isotope mass spectrometer, MAT253, Thermo Fisher Scientific, United States), and the detection limit was 0.2×10^{-9}. The analysis of the stable carbon isotopes of methane is based on the standard of "Method for Organic Geochemical Analysis of Geological Samples" (GB/T 18340.2-2010). The results were given relative to the PDB ‰.

Samples of the source rock were analyzed at the Yangtze University, and its main test indicators include total organic carbon (TOC), Rock-Eval, chloroform bitumen "A," concentrations of kerogen element, and vitrinite reflectance (*Ro*). Among all these indicators, the test reference is GB/T19145-2003, GB/T18602-2012, SY/T5118-2005, SY/T5122-1986, and SY/T5154-2012, respectively. TOC was measured by infrared carbon–sulfur determination (Carbon and sulfur analyzer, CS-230, Leco Corporation, United States), and the test conditions were temperature 17.6 °C and humidity 39%. Rock-Eval was measured by using a rock pyrolysis analyzer (OGE-II, Research institute of petroleum exploration development, China), and the test conditions were temperature 17.7 °C and humidity 39%. Chloroform bitumen "A" was measured by accelerated solvent extraction (ASE, ASE200, Thermo Fisher Scientific, United States). The concentrations of kerogen elements were measured by an organic element analyzer (CE-440, accuracy, 0.15%, Exeter Analytical Incorporated, United States). *Ro* was measured by using a vitrinite reflectance tester (DMLP with MSP200, J&M Analytik AG, Germany), and the test conditions were temperature 23°C and humidity 50%. The aforementioned data received the acceptance of the quality inspection center for geochemical sample analysis of CGS, and the analysis quality is reliable.

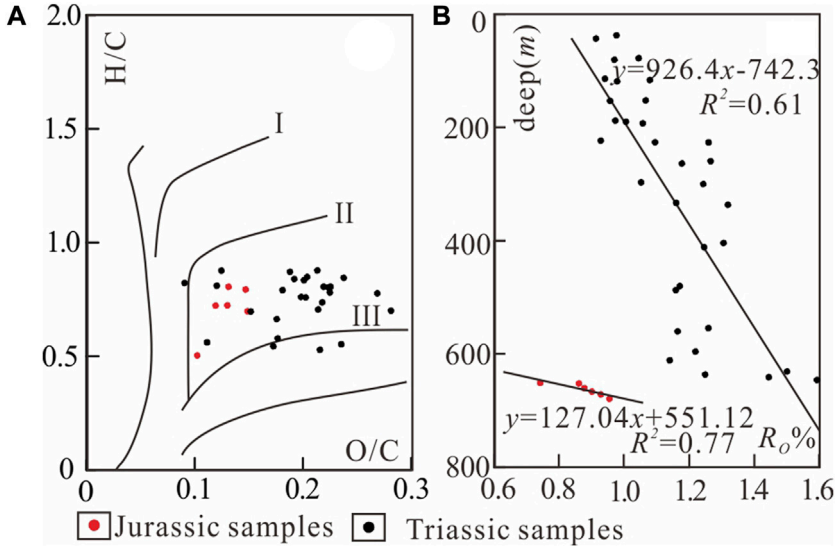

FIGURE 2
(A) O/C versus H/C of the samples from the DK 12–13 core in the Qilian Mountain permafrost. **(B)** Variation of R_O with the depth of the samples from the DK 12–13 core in the Qilian Mountain permafrost.

4 Results and discussion

4.1 Gas sources

Since the discovery of NGH in the Muli region of Qilian Mountain permafrost, domestic experts have attained remarkable achievements in related research on gas sources. Yet, the consensus has not been reached. There are three main different opinions: 1) its gas source is the product from the thermal evolution in the dispersed organic matter within coal seams. Also, its formation is associated with coal seams and mainly comes from coal-seam gas (Lu et al., 2011, 2013; Dai et al., 2014); 2) its gas mainly originates from pyrolysis gas, with oil-associated gases and condensate-associated gas so that it has less connection with the coal-seam gas (Lu et al., 2020); 3) its gas source is a mixed gas. For coal-seam gas, its source comes from the Jurassic coal seams while oil-associated gas may come from the underlying upper Triassic Galedesi formation or even further (Huang et al., 2016).

4.1.1 Organic matter abundance

Organic matter abundance is a critical index to measure the hydrocarbon generating capacity. There are a total of 40 organic carbon samples in this test, of which six samples are from the Middle Jurassic Muli formation, with a sampling depth of 630.50–679.10 m. Also, other 34 suites in the Upper Triassic Galedesi formation also have been tested with the depth of 37.52–610.5 m. The results show that more than 80% of hydrocarbon source rocks in both formations have organic carbon concentration over 1%. The Muli formation (J_2m) has TOC, hydrocarbon generation potentials (S_1+S_2), and maximum pyrolysis temperature (Tmax) values in the range of 0.47–1.78%, 0.21–6.18 mg/g, and 452–461°C, with average values of 1.28%, 3.40 mg/g, and 456°C, respectively. Half samples are the best source rocks, and over 83.33% are the good ones. Meanwhile, the Galedesi formation (T_1g), has TOC, S_1+S_2, and Tmax values in the range of 0.05–1.39%, 0.21–6.18 mg/g, and 465–537°C, with average values of 1.32%, 0.58 mg/g, and 472°C, respectively. Therefore, it is obvious that hydrocarbon generation potential in both strata is good (Table 1). Also, the results also demonstrate the source rocks in the Middle Jurassic Muli formation are evaluated as good ones as they have more chloroform bitumen "A," with their concentration in all six samples being over 0.015 and 66.67% of them being over 0.1%. The source rocks in the Upper Triassic Galedesi formation are assessed as bad ones and non-generating carbonate rocks because the concentration of "A" in most samples is less than 0.05% (Table 1).

4.1.2 Organic matter type

Organic matter type is a parameter to examine the organic hydrocarbon generating capacity and determine its products to be oil-orient or gas-orient. Kerogen type Ⅰ owns the primitive H/C atomic ratio at a higher level while the O/C at a lower level, with high hydrocarbon generation potential and forming mainly oil. Kerogen type Ⅱ has hydrocarbon generation potential amount that is in a medium level and is yet to be a good source rock. Then, Kerogen Type Ⅲ hydrocarbon generation potential is small, which produces mainly gas (Lu and Zhang,

TABLE 2 Gas components and carbon isotope composition of gas hydrates found in the Qilian Mountain permafrost.

Well number	Well depth/m	Components/μl/L					C_1/C_2+C_3	$\delta^{13}C$ CH_4(‰, VPDB)
		CH_4	C_2H_6	C_3H_8	C_4H_{10}	C_5H_{12}		
DK-8	148–154	21,368	2,238	1,136			4.47	−44.38
	166–167	85,628	23,973	8,386	620	304	3.57	−44.30
	173–175	148,858	40,700	18,682	1,456	631	3.56	−44.40
	225–227	148,607	29,871	20,308	1795	724	4.75	−46.08
	230–240	184,684	43,342	29,033	2,574	1,144	3.85	−45.11
	266–287	339,621	54,859	31,845	2,527	1,212	6.10	−47.16
	289–291	278,364	38,349	19,957	1841	918	7.11	−49.76
DK13-11	130,327	115,283	47,188	24,196	859	419	1.98	−44.20
DK12-13	129–274	119,889	51,192	31,281	1,171	445	2.07	-43.60

2008). In the research area, the average O/C atomic ratio of the source rocks in the Middle Jurassic Muli formation is 0.13, and the average ratio of the Upper Triassic Galedesi formation is 0.20. There are great differences between the figures of the two strata, yet the figures for the H/C atomic ratio have a minor difference of 0.71 and 0.75, respectively. The main kerogen types in Middle Jurassic Muli formation are II_2, II_1, and III and II_1 in Upper Triassic Galedesi formation, with few samples being the kerogen type I (Figure 2A).

4.1.3 Organic matter evolution

Organic matter maturity is a significant index to determine the process when organic matters become gas. It is suggested by vitrinite reflectance (*Ro*) that all the values of these samples are over 0.68%. In the study area, the *Ro* of the source rocks in the Middle Jurassic Muli formation is 0.68–1.27%, indicating they have reached the mature stage of organic matters and the peak of generating oil, which can be called the forming stage of crude oil along with immense oil-associated gas. Meanwhile, the *Ro* of the source rocks in the Upper Triassic Galedesi formation is 1.04–1.81%, indicating the highly mature stage of organic matter. Such rocks can produce hydrocarbon products consisting mainly of light hydrocarbon (C_1–C_5) with lower relative molecular mass. Then, both *Ro* values show good linear relativity with the depth (Figure 2B), with the correlation coefficient of R^2 being 0.77 and 0.61, respectively, which shows that having been buried and experiencing higher paleogeothermal activity leads to higher stratum maturity. However, it is difficult to determine the accurate time when the highest paleogeothermal activity happened simply by taking advantage of the *Ro* analysis.

Generally speaking, the concentrations of organic carbon in both formations are at a higher level, but the types of organic matter are different from each other. The coal-bearing rocks in the Middle Jurassic Muli formation consisted mainly of types II_1 and II_2. As for the Upper Triassic Galedesi formation, its coal-bearing rocks are mainly constituted by types III and II_1 at the mature stage to produce gas. It is also indicated from the comparison of each oil source that the Middle Jurassic oil-contained seams in the DK-9 well come from the hydrocarbon source rock in the Middle Jurassic times (Cheng et al., 2018). The Upper Triassic kerogen is at a high-mature stage yet with less hydrocarbon generating capacity, but its products are mainly light hydrocarbons, providing stable gas resources for the NGH.

4.1.4 Gas genetic type

There are 500 rock core samples in total respectively from well DK-8, DK11-13, and DK13-12. Also, 400 samples collected from DK-8 well have been examined where the $\delta^{13}C_1$ is over −50‰ and its average is −47.41‰, which are featured with pyrolysis and mixture gas, respectively. Its R (dry coefficient, R = C1/(C2+C3)) value is lower at 100 and average at 13.70. Also, in the 56 samples from DK11–13, the $\delta^{13}C_1$ of these samples is over −50‰, and its average is −43.60‰ (Table 2), which are the typical characteristic of pyrolysis gas, with its R being lower than 100 (Figure 3A). In the 44 samples from DK13–12, the $\delta^{13}C_1$ of these samples is over −50‰, and its average is −44.20‰ (Table 2), which are the typical characteristic of pyrolysis gas, with its R being lower than 100 (Figure 3A). Meanwhile, they contain more methane and heavy hydrocarbon (including ethane, propane, and butane), featuring wet gas. Based on the identification chart (Dai, 1993; Whiticar, 1999), this research casts the $\delta^{13}C_1$ and R into the chart (Figure 3B). It is obvious that the dotted area of wells DK-8, DK11-13, and DK13-12 is basically in the same shape, producing mainly oil-associated gases, condensate-associated gas, and coal-seam gas.

According to the geochemical evaluation method of terrestrial source rocks (SY/T 5735–1995), the hydrocarbon source rocks in the Middle Jurassic Muli formation and Upper Triassic Galedesi formation are examined as good ones, in which the former rocks are at the mature stage of organic

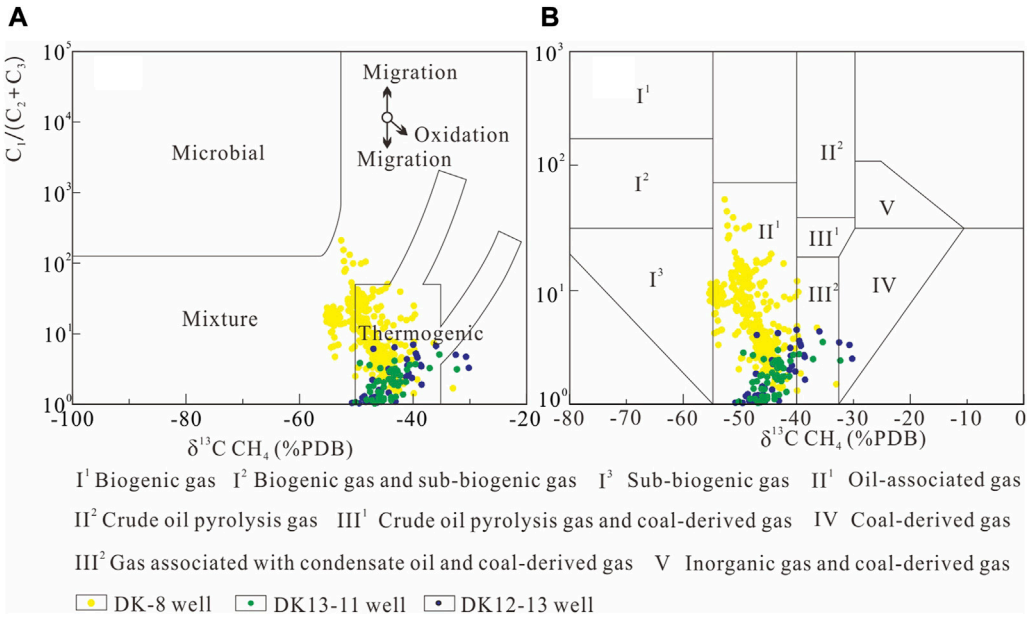

FIGURE 3
(A) Relationship between methane carbon isotope composition vs. ethane and propane molecular composition (modified after Whiticar, 1999).
(B) $\delta^{13}C_1$-C_1/C_{2+3} identification plate (modified after Dai, 1993).

matters and the peak of generating crude oil with immense petroleum-associated gas. Also, the rocks in the Upper Triassic are in a high-mature stage to produce more gas, offering efficient gas for the NGH, symbolizing the multi-sources of the NGH in Qilian Mountain.

4.2 Hydrocarbon generation history

There are several suites of hydrocarbon source rocks developed in the Southern Qilian Basin that are rendered as superior ones with promising hydrocarbon generation potential, reaching mature to the over-mature stage, including the Carboniferous mudstone, black limestone in the Lower Permian Caodigou formation, black mudstone in the Upper Triassic Galedesi formation, and the oil shale in the Middle Jurassic Muli formation (Fu and Zhou, 2000). Based on PetroMod basin simulation software, this research has calculated the hydrocarbon generation history in the target area.

According to the global standard stratigraphic age, stratigraphic burial history simulation adopts the interpolation methods to attain the modeling stratigraphic age with the sequence of geological time scale. Also, the data of buried depth of the top and bottom of strata and lithology are built by the field observation. Then, the geothermal history simulation adopts the stable constant thermo-fluid model, while the mature history simulation uses the first-level reaction model of Easy *Ro*% kinetics established by Sweeney to observe the evolution history of each hydrocarbon-generating stratum. Also, hydrocarbon generating history stimulation takes advantage of the Kerogen–oil–gas model provided by the software. The paleo-depth is mainly analyzed from the deposition at that period and contemporary sedimentary water depth to establish the relative standards (2–10 m for a continental deposit and 50–100 m for a marine deposit). The interface temperature of sedimentary water is attained by the comprehensive calculation of paleotemperature and water depth. It is demonstrated by the hydrocarbon generating history research that the hydrocarbon source rocks in the bottom of the Muli formation have reached the hydrocarbon generation threshold (R_o = 0.5%) in early Cretaceous (around 140 Ma) and entered the mature stage of thermal evolution (R_o > 0.7%) in later Cretaceous (100 Ma), now at the near peak of hydrocarbon generation (R_o = 1.0%). As for the bottom rock in the Galedesi formation, it reached the hydrocarbon generation threshold (R_o = 0.5%) in the early Jurassic (190–180 Ma) and entered the same mature stage (R_o > 0.7%) in the Middle Jurassic (165 Ma), naming the peak stage of hydrocarbon generation. Then, in the early Late Cretaceous (90–100 Ma), it achieved the highly mature stage of thermal evolution. Presently, the bottom rock in the Galedesi formation is in the highly mature stage of thermal evolution, while its top is around the peak of hydrocarbon generation (R_o = 1.0%). The whole rocks in this formation are at the thermal evolution from the mature to the over-mature stage, with considerable hydrocarbon generation potential (Figure 4).

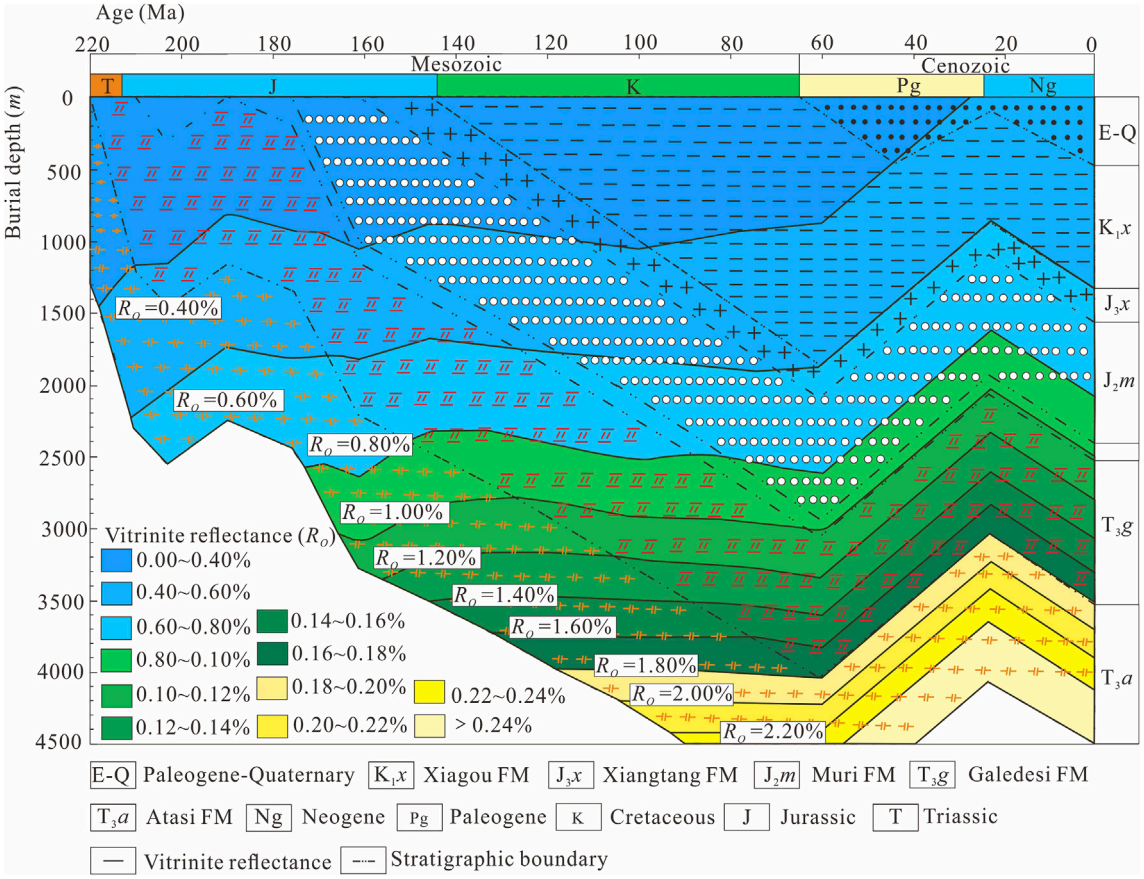

FIGURE 4
Hydrocarbon generation history of the Muri depression in Qilian Mountain.

4.3 Gas migration

Hydrocarbon gas through some migration ways, such as crack and fracture, plays a key role in forming the NGH reservoir (Boswell et al., 2011). Jurassic systems in the study area and stratum fold in the underlying Late Paleozoic–Mesozoic have formed north syncline structures in an extensive, wide, and gentle way (Wen et al., 2011). In the process of forming a buckle fold, there is a series of bedding shear joints and interlayer fracture zones. At the same time, there are conjugate joints in settings of tectonic stress fields with near north–south orientation (Wen et al., 2011). All those fracture zones, bedding shear joints, micro-fissures, and rock pores (especially pores in coarse clastic rocks above the unconformity) provide a pathway for hydrocarbon migration. Generally speaking, methane in the NGH comes from the transformation of organic matter under the effect of microorganisms or methane-bearing fluid from deep migration. In addition, as an ideal pathway for deep fluid, fault structure attracts much attention. The NW–SE thrust faults (F_1 and F_2) were formed from the Late Middle Jurassic to the early Cretaceous in the study area and are the most important faults in the study area. DK-8 well logging data show that anomalies associated with gas hydrates occurred at depths of 144.4–152.0 m and 235.0–291.3 m, and the profile has produced F_1 and F_2 footwall faults (Lu et al., 2015); all those features show that NGH is obviously controlled by F_1 and F_2 thrust structure, where higher gas concentrations were found in the headspace gases. At 155–167 m and 235–310 m, the concentration curves of methane, ethane, ethylene, and propane show large peaks, while R values have a small peak (Figure 5), which suggests the presence of an invisible and pervasive gas hydrate at this interval. The DK8 well (131.4–386.4 m) with high headspace gas concentration produces many fracture zones, and the core develops fracture and fault (Table 3). It is shown that hydrocarbon gases move upward along with faults and fracture zones (Figure 5), which have many abnormal layers of NGH and provide a pathway for migration of deep gases. Shallow faults and fractures are gas sources and storage space for NGH self-source and self-reservoir.

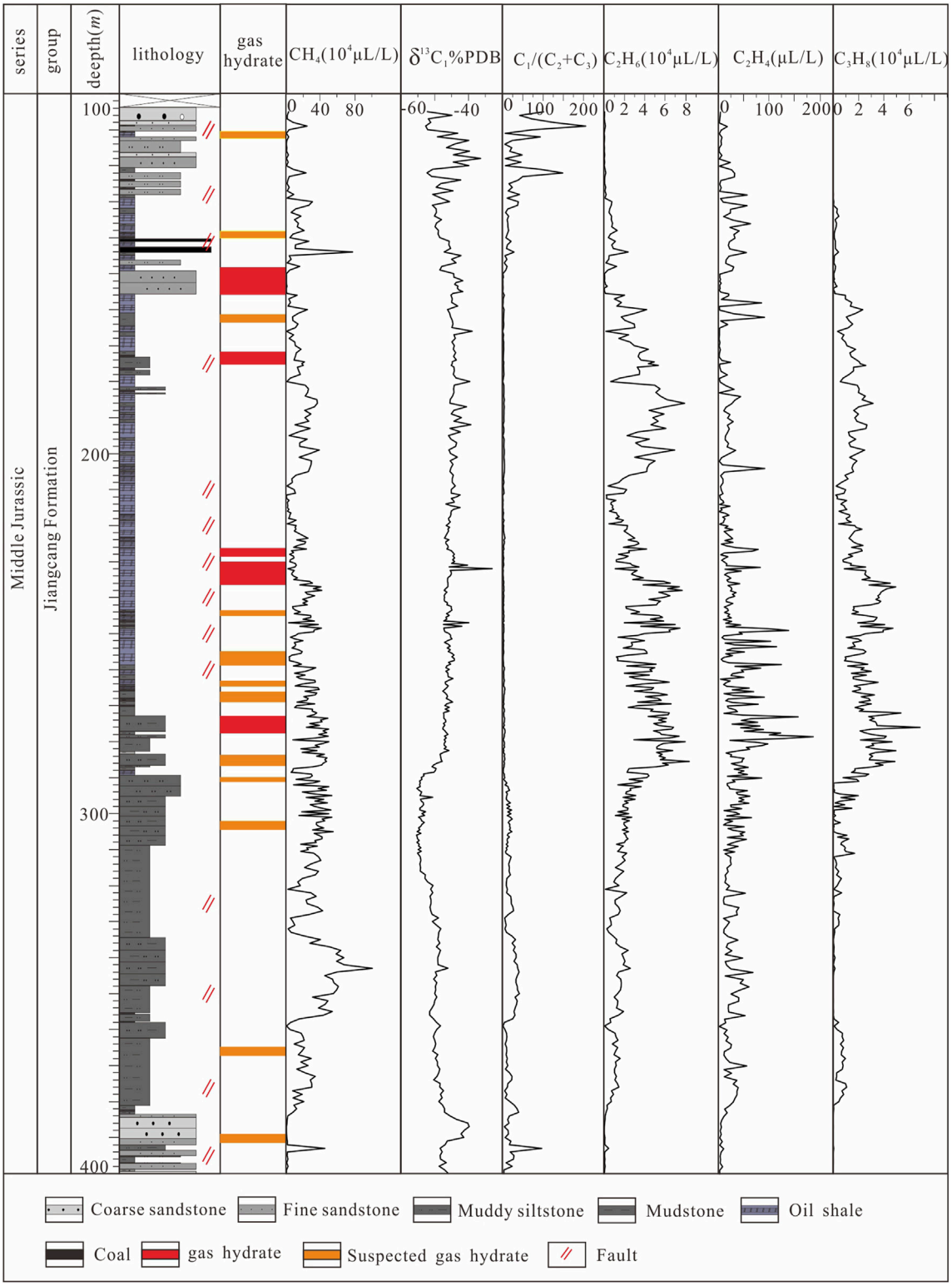

FIGURE 5
Variation of gas concentrations and methane stable isotopes with depths in headspace gases from the DK-8 core in the Qilian Mountain permafrost.

TABLE 3 Characteristics of faults or fractures observed in the drill core of well DK-8 in the Qilian Mountain permafrost.

Depth	Lithology	Characteristics
107.60–108.70	Whitish	Small obvious fault at 107.9 m, inter-bedded with thin coal
27.51–127.81	Fault gouge	Consisting of mud and gravels, fractured, and striation
149.33–149.60	Fault gouge	Fractured, mud mixed with sand and gravel
176.69–176.84	Siltstone inter-bedded with oily shale	Striation on fracture surface of upper sandstone, fractured oil shale, and siltstone on the lower section
221.06–221.21	Fault gouge	Fractured, including silt mud pebble
221.46–223.06	Fracture zone	Fractured, no unbroken core
37.85–238.11	Fault gouge	Mixture of mud, mud pebble, shale, and gravel
240.66–240.90	Fault gouge	Mixed mud, mud pebble, and oil shale fragments
259.66–260.01	Fault gouge	Mixed mud pebble and oil shale fragments
331.80–332.10	Argillaceous siltstone	Striations on local fracture surface
355.65–358.00	Grey black silty mudstone	Striations on fracture surface
381.10–382.40	Grey black mudstone	Fractured, striations on the fracture surface
397.15–399.80	Grey white fine sandstone	Vertical fissures, oil stains of the heavy hydrocarbon on fracture surface on 397.73 m

4.4 Trap and cap rock

A trap is a necessary condition for forming an NGH reservoir (Collett and Dallimore, 2003; Makogon, 2010; Boswell et al., 2011; Collett et al., 2011). For example, on the north slope of Mount Elbert in Alaska, its NGH reservoir has, under the combined control of structure and lithologic trap (Boswell et al., 2011); NGH in Mackenzie, the north of Canada, also aggregated in the anticlinal ridge or the uplift part of the large anticline or the saturation of the reservoir rising toward the uplift part (Majorowicz and Osadetz, 2001). In addition, NGH in Mallik is also controlled by structure and lithologic traps (Dallimore and Collett, 2005). The NGH of the permafrost in the Qilian Mountain is mainly produced from the layer section of mudstone, oil shale, siltstone, and fine sandstone, and it has little to do with lithology. Its NGH often appears in the fracture and pores of rocks. Therefore, the NGH in Qilian Mountain is obviously controlled by structural traps (Wang et al., 2014).

The NGH from the Muli area in Qilian Mountain is under permafrost. A number of measured data show that the thickness of the permafrost in Qilian Mountain is 8.0–139.3 m and that thickness in the Muli area is 60–95 m (Zhou et al., 2000). Results of a thermometric study from DK-9 show that the thickness of permafrost in the drilling region is about 95 m, the NGH is produced under 133 m (Zhu et al., 2010), and the permafrost on the top is a kind of geologic body with much lower permeability and higher sealing. Research shows that permeability is decreasing along with the increase in ice saturation degree. When the degree of ice saturation reaches 50 percent, methane gas permeability is decreasing sharply; when the former comes to 60 percent, the latter decreases to 1 percent of the initial value; when the former comes to 80 percent, the latter decreases to a millionth of the initial value, which is to say it approaches zero (Wang et al., 2015). Therefore, permafrost is likely to prevent its lower free gas from moving upward and accumulating and become a necessary cap rock for the forming of NGH.

4.5 Natural gas hydrate formation time

The NGH stability zone is delineated by the temperature pressure phase equilibrium curve and geothermal gradient curve, which can predicate the range of the NGH (Zhu et al., 2011). A stability zone is necessary for the formation of the NGH and Tundra is one of the key factors to determine a stability zone. Qilian Mountain is located in the middle latitudes of China, so its temperature is higher than that in high-latitude and polar areas, and its snow line is also quite higher. The forming of permafrost needs a coupling effect of global cooling and the tectonic uplift. Therefore, the development of permafrost in Qilian Mountain is mainly determined by the altitude of the mountain. According to geomorphological and sedimentological evidence, the most intense uplift of Qilian Mountain starts from the Qinghai–Tibet movement of 3.6 Ma, Kunlun–Yellow River tectonic movement of 0.8–1.2 Ma comes to the critical height of 3,000 m required for glaciation, and the Gonghe movement of 150 ka lifted the mountain to its present height (Cui et al., 1997; Li and Fang, 1998). The Qinghai–Tibet Plateau comes to the cryosphere by rapidly uplifting, which brings a drastic change to its environment and then comes out with the biggest glacier since the Quaternary (Li, 2013). Until now, the biggest glacier is found in a stable environment. The formation time of the permafrost in Qilian Mountain is not earlier than about 1.2 Ma. The stable zone will be formed after the formation of the Tundra, and the NGH will be formed in an environment with sufficient gas source supplies, good gas components, and reservoir characteristics in the stability zone.

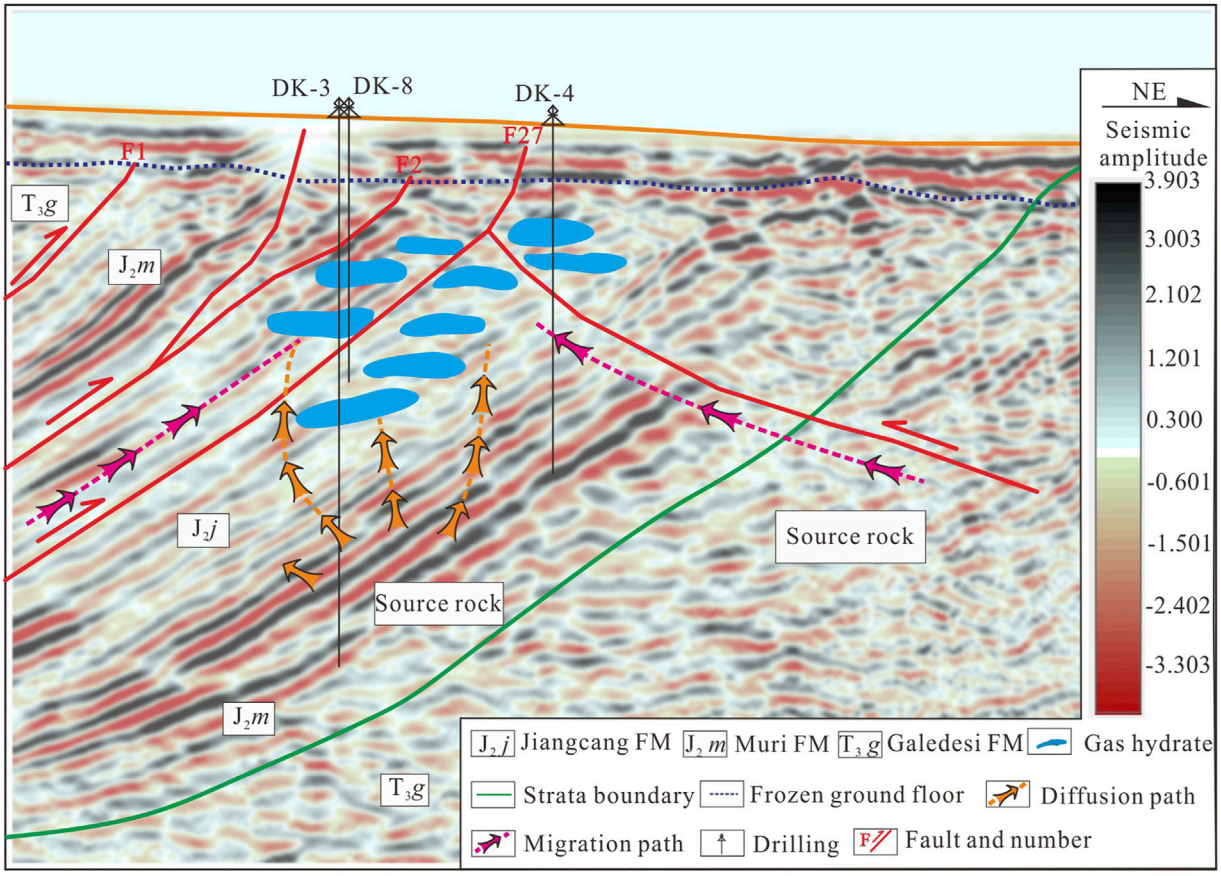

FIGURE 6
Mechanism for NGH accumulation in Qilian Mountain permafrost.

5 Accumulation mechanism

Based on the analysis of geology and geochemistry, the accumulation mechanism of the NGH in Qilian Mountain permafrost has been initially established, which is similar to the pattern of clathrates of conventional gas reservoirs summarized by Beauchamp (Beauchamp, 2004). Gas hydrate in the Qilian Mountain permafrost was formed under a series of complicated processes, including gas generation, gas migration and accumulation, and gas hydrate formation. The gas source of NGH in the permafrost of Qilian Mountain is mainly the oil-associated gas and includes a small amount of condensate-associated gas, kerogen cracking gas, and others, while in the study area, it mainly comes from hydrocarbon source rocks of the Middle Jurassic Muli formation and Upper Triassic Galedesi formation (Figure 6).

During Early Jurassic to Late Cretaceous, the study area is in the subsidence period (Cui et al., 1997). At the end of the Early Cretaceous, the buried depth of mudstone in the Upper Triassic and coal-bearing mudstone in the Middle Jurassic was approximately 3,000 m, and its forming temperature was up to 120°C, which were beneficial for producing gases (Li and Fang, 1998; Jiang et al., 2015). Hydrocarbon formation history shows that hydrocarbon source rocks of the Galedesi formation in the Middle Jurassic (165 Ma) come to the mature thermal evolution stage with a hydrocarbon generation peak, while for Muli formation, they reach the hydrocarbon generation threshold in the Early Cretaceous (about 140 Ma). The two kinds of hydrocarbon source rocks mentioned earlier in the Late Cretaceous (100–90 Ma) come into the high mature and mature thermal evolution stage, respectively. Petroliferous pyrolysis gases from hydrocarbon source rocks in the Galedesi formation start the primary migration, and the newly formed oil and gas in the Muli formation in the Early Cretaceous start migrating for the first time. They aggregate into a reservoir from hydrocarbon source rocks.

During the Late Middle Jurassic to the Early Cretaceous, the Yanshan movement uplifted and eroded the study area, and NW–SE thrust faults were formed in this area (Figure 1). The thrust faults of F_1 and F_2 formed at a relatively late stage of this period and were characterized by continuous compression and effective sealing properties for gas migration (Lu et al., 2013;

Chen et al., 2015). The thermogenic gas entered into different fracture zones or rock fractures during gas migration from deep reservoirs to shallow layers from deep reservoirs along faults of F_1 and F_2 (Figure 6). The faults of F_1 and F_2 played a role in the migration pathway and effective plugging for gas in gas hydrate formation. The tight and complete mudstone and oil shale above the fracture zone acted as cap rocks. The gas accumulation zone was formed in fractured reservoirs.

In the Miocene, the Kunhuang movement makes the study area uplift to a critical height above 3,000 m required for glaciation (Li and Fang, 1998). The Gonghe movement lifted the mountain to its present height, and the study area comes into the cryosphere by rapidly uplifting (Jiang et al., 2015). The oil and gas might have secondary migration, and the tight mudstone and oil shale above the fracture zone provide the capping rock. In the upper part of the Middle Jurassic Muli formation, fractured reservoirs such as mudstone, oil shale, and siltstone formed the natural gas accumulation zone. In the meanwhile, the Muli formation has also at the peak of hydrocarbon generation generating hydrocarbon gas continuously. The addition of ethane, propane, carbon dioxide, and coal-seam gas lowers the temperature and pressure conditions for NGH formation (Lu et al., 2015), and then the NGH comes into being during this period. The NGH was formed under the combined control of sedimentation, paleoclimate, tectonic movement, and other factors.

According to the previous description, the mechanism of gas hydrate formation in this area can be summarized as follows: gas generation and migration controlled by tectonic subsidence, accumulation controlled by faults, and accumulation controlled by permafrost. The tectonic uplift in Qilian Mountain lifts the deep gas to the near surface and provides a suitable temperature for NGH formation, which is the result of the coupling effect of tectonics and climate. The formation of the NGH in Qilian Mountain underwent three phases, including gas migration and accumulation during the Late Jurassic to Early Cretaceous, overall uplift from the Middle and Late Miocene to Pliocene, and transformation from free gas to the NGH in the Quaternary. It has undergone the process of "aggregation first—then uplift—finally accumulation."

6 Conclusion

1) NGH in the Qilian Mountain permafrost shows the domination of pyrolysis gas, with oil-associated gas as its majority and coal-seam gas as its minority. Both hydrocarbon source rocks in the Middle Jurassic Muli formation and Upper Triassic Galedesi formation rank as relatively good source rocks and converge together along faults and fractures through diffusion and migration, respectively, so as to provide sufficient gas supply for NGH, showing characterized by multi-source and multi-stages.
2) The drilling research in Qilian Mountain permafrost suggests that the NGH layer reserves show relatively high methane concentration and organic carbon concentration and relatively low dry coefficient, featuring with wet gas. Many fracture zones precisely develop in the interval on the drilling core with high headspace gas concentrations, which indicates that the fault or fracture zone is the pathway of hydrocarbon gas migration.
3) According to the geological and geochemical analysis, the accumulation mechanism of the NGH in Qilian Mountain permafrost has been initially established. The formation of the NGH in Qilian Mountain underwent three phases, namely, gas migration and accumulation during Late Jurassic to Early Cretaceous, overall uplift from the Middle and the Late Miocene to Pliocene, and transformation from free gas to the NGH in the Quaternary. It has undergone the process of "aggregation first—then uplift—finally accumulation," which is the result of the coupling effect of tectonics and climate.

Data availability statement

The original contributions presented in the study are included in the article/supplementary material; further inquiries can be directed to the corresponding author.

Author contributions

FZ: conceptualization and writing—reviewing and editing. ZY: conceptualization, resources, and supervision. YZ: writing—original draft preparation. SZ: writing—reviewing. LY: editing and investigation.

Funding

This work was funded by China Geological Survey Project (Nos. AS2016Y01, DD20160224, and AS2019J02).

Conflict of interest

The authors declare that the research was conducted in the absence of any commercial or financial relationships that could be construed as a potential conflict of interest.

Publisher's note

References

Beauchamp, B. (2004). Natural gas hydrates: Myths, facts and issues. *Comptes Rendus Geosci.* 336 (9), 751–765. doi:10.1016/j.crte.2004.04.003

Boswell, R., Collett, T. S., Frye, M., Shedd, W., McConnell, D. R., and Shelander, D. (2012). Subsurface gas hydrates in the northern Gulf of Mexico. *Mar. Petroleum Geol.* 34 (1), 4–30. doi:10.1016/j.marpetgeo.2011.10.003

Boswell, R., Moridis, G., Reagan, M., and Collett, T. S., "Gas hydrate accumulation types and their application to numerical simulation," in United Kingdom: Proceedings of the Seventh International Conference on Gas Hydrate, Edinburgh, Scotland, 2011.

Chen, L. M., Cao, D. Y., Jiang, A. L., Qin, R., Li, J., Li, Y. H., et al. (2015). Structural control of reservoir forming for natural gas hydrate in Sanlutian well field, Qinghai. *Sci. Technol. Rev.* 33 (6), 91–96. doi:10.3981/j.issn.1000-7857.2015.06.015

Cheng, B., Xu, J. B., Lu, Z. Q., Li, Y., Wang, W., Yang, S., et al. (2018). Hydrocarbon source for oil and gas indication associated with gas hydrate and its significance in the Qilian Mountain permafrost, Qinghai, Northwest China. *Mar. Petroleum Geol.* 89, 202–215. doi:10.1016/j.marpetgeo.2017.02.019

Collett, T. S., Boswell, R., Waite, B. W., Kumar, P., Roy, S. K., Chopra, K., et al. (2019). India national gas hydrate program expedition 02 summary of scientific results: Gas hydrate systems along the eastern continental margin of India. *Mar. Petroleum Geol.* 108, 39–142. doi:10.1016/j.marpetgeo.2019.05.023

Collett, T. S., and Dallimore, S. R. (2003). *Permafrost-associated gas hydrate natural gas hydrate*. Dordrecht, Netherlands: Springer Netherlands, 43–60.

Collett, T. S., Lee, M. W., Agena, W. F., Miller, J. J., Lewis, K. A., Zyrianova, M. V., et al. (2011). Permafrost–associated natural gas hydrate occurrences on the Alaska North Slope. *Mar. Petroleum Geol.* 28 (2), 279–294. doi:10.1016/j.marpetgeo.2009.12.001

Collett, T. S. (1994). Permafrost–associated gas hydrate accumulations. *Ann. N. Y. Acad. Sci.* 715 (1), 247–269. doi:10.1111/j.1749-6632.1994.tb38839.x

Cui, Z. J., Wu, S. Q., and Liu, G. N. (1997). Discovery and properties of Kunlun Yellow River movement. *Chin. Sci. Bull.* 42 (18), 1986–1988.

Dai, J. X., Ni, Y. Y., Huang, S. P., Liao, F. R., and Wu, W. (1993). Hydrocarbon isotopic characteristics and identification of various types of natural gas. *Nat. Gas. Geosci.* 4 (2–3), 1–40.

Dai, J. X., Ni, Y. Y., Huang, S. P., and Liao, F. R., (2014). Significant function of coal-derived gas study for natural gas industry development in China. *Nat. Gas. Geosci.* 25 (1), 1–22. doi:10.11764/j.issn.1672-1926.2014.01.0001

Dallimore, S. R., and Collett, T. S. (2005). Scientific results from the Mallik 2002 gas hydrate production research well program, Mackenzie Delta, Northwest Territories, Canada. *Bull. Geol. Surv. Can.* 585, 140. doi:10.4095/220702

Fang, H., Xu, M. C., Lin, Z. Z., Zhong, Q., Bai, D., Liu, J., et al. (2017). Geophysical characteristics of gas hydrate in the Muli area, Qinghai Province. *J. Nat. Gas Sci. Eng.* 37, 539–550. doi:10.1016/j.jngse.2016.12.001

Farahani, M. V., Hassanpouryouzband, A., Yang, J. H., and Tohidi, B. (2021b). Development of a coupled geophysical-geothermal scheme for quantification of hydrates in gas hydrate-bearing permafrost sediments. *Phys. Chem. Chem. Phys.* 23 (42), 24249–24264. doi:10.1039/d1cp03086h

Farahani, M. V., Hassanpouryouzband, A., Yang, J. H., and Tohidi, B. (2021a). Insights into the climate-driven evolution of gas hydrate-bearing permafrost sediments: Implications for prediction of environmental impacts and security of energy in cold regions. *RSC Adv.* 11 (24), 14334–14346. doi:10.1039/d1ra01518d

Fu, J. H., and Zhou, L. F. (2000). Triassic stratigraphic provinces of the southern Qilian basin and their petro-geological features. *Northwest Geosci.* 21 (2), 64–72.

Hassanpouryouzband, A., Joonaki, E., Farahani, M. V., Takeya, S., Ruppel, C., Yang, J., et al. (2020). Gas hydrates in sustainable chemistry. *Chem. Soc. Rev.* 49 (15), 5225–5309. doi:10.1039/c8cs00989a

Hesselbo, S. P., Groecke, D. R., Jenkyns, H. C., Bjerrum, C. J., Farrimond, P., Morgans Bell, H. S., et al. (2000). Massive dissociation of gas hydrate during a Jurassic oceanic anoxic event. *Nature* 406, 392–395. doi:10.1038/35019044

Huang, X., Liu, H., Zhang, J. Z., Wang, P. K., and Zhu, Y. H., (2016). Genetic-type and its significance of hydrocarbon gases from permafrost-associated gas hydrate in Qilian Mountain. *Chin. J. Geol.* 51 (3), 934–945. doi:10.12017/dzkx.2016.039

Jiang, A. L., Chen, L. M., Qin, R. F., Jiang, L. I., and Cao, D. Y., (2015). Tectonic subsidence history of Sanlutian mining field in Muli, Qinghai. *Geomechanics* 21 (3), 1096–1102. doi:10.3969/j.issn.1000-8527.2015.05.011

Katz, M. E., Pak, D. K., Dickens, G. R., and Miller, K. G. (1999). The source and fate of massive carbon input during the Latest Paleocene Thermal Maximum. *Science* 286 (5444), 1531–1533. doi:10.1126/science.286.5444.1531

Kennedy, M., Mrofka, D., and Borch, C. V. D. (2008). Snowball Earth termination by destabilization of equatorial permafrost methane clathrate. *Nature* 453 (7195), 642–645. doi:10.1038/nature06961

Konno, Y., Fujii, T., Sato, A., Akamine, K., Naiki, M., Masuda, Y., et al. (2017). Key findings of the world's first offshore methane hydrate production test off the coast of Japan: Toward future commercial production. *Energy fuels.* 31 (3), 2607–2616. doi:10.1021/acs.energyfuels.6b03143

Kvenvolden, K. A. (1993). Gas hydrates-geological perspective and global change. *Rev. Geophys.* 31 (2), 173–187. doi:10.1029/93rg00268

Lee, M. W., and Collett, T. S. (2013). Characteristics and interpretation of fracture-filled gas hydrate - an example from the ulleung basin, east sea of korea. *Mar. Petroleum Geol.* 47, 168–181. doi:10.1016/j.marpetgeo.2012.09.003

Li, B., Sun, Y. H., Guo, W., Shan, X., Wang, P., Pang, S., et al. (2017). The mechanism and verification analysis of permafrost-associated gas hydrate formation in the Qilian Mountain, Northwest China. *Mar. Petroleum Geol.* 86, 787–797. doi:10.1016/j.marpetgeo.2017.05.036

Li, J. F., Ye, J. L., Qin, X. W., Qiu, H. J., Wu, N. Y., Lu, H. L., et al. (2018). The first offshore natural gas hydrate production test in South China Sea. *China Geol.* 1 (1), 5–16. doi:10.31035/cg2018003

Li, J. J., and Fang, X. M. (1998). Study on uplift and environmental change of Qinghai-Tibet plateau. *Chin. Sci. Bull.* 43 (15), 1569–1574.

Li, J. J. (2013). Qinghai-Tibet plateau uplift and late Cenozoic environmental changes. *J. Lanzhou Univ. Nat. Sci.* 49 (2), 5–8. doi:10.3969/j.issn.0455-2059.2013.02.002

Liang, J. Q., Zhang, W., Lu, J. A., Wei, J., Kuang, Z., and He, Y. (2019). Geological occurrence and accumulation mechanism of natural gas hydrates in the eastern Qiongdongnan Basin of the South China Sea: Insights from site GMGS5-W9-2018. *Mar. Geol.* 418, 106042. doi:10.1016/j.margeo.2019.106042

Lin, Z. Z., Pan, H. P., Fang, H., Gao, W., and Liu, D. (2018). High-altitude well log evaluation of a permafrost gas hydrate reservoir in the Muli area of Qinghai, China. *Sci. Rep.* 8 (1), 12596. doi:10.1038/s41598-018-30795-x

Lu, S. F., and Zhang, M. (2008). *Oil and gas geochemistry*. Beijing: Petroleum industry press.

Lu, Z. Q., Tang, S. Q., Luo, X. L., Zhai, G. y., Fan, D. w., Liu, H., et al. (2020). A natural gas hydrate-oil-gas system in the Qilian Mountain permafrost area, northeast of Qinghai-Tibet Plateau. *China Geol.* 3 (4), 511–523. doi:10.31035/cg2020075

Lu, Z. Q., Li, Y. H., Wang, W. C., Liu, C. L., and Wen, H. J., (2015). Study on the accumulation pattern for permafrost-associated gas hydrate in Sanlutian of Muli, Qinghai. *Geoscience* 29 (5), 1014–1023. doi:10.3969/j.issn.1000-8527.2015.05.004

Lu, Z. Q., Zhu, Y. H., Liu, H., Zhang, Y., Jin, C., Huang, X., et al. (2013). Gas source for gas hydrate and its significance in the Qilian Mountain permafrost, Qinghai. *Mar. Petroleum Geol.* 43, 341–348. doi:10.1016/j.marpetgeo.2013.01.003

Lu, Z. Q., Zhu, Y. H., Zhang, Y. Q., Wen, H., Li, Y., and Liu, C. (2011). Gas hydrate occurrences in the qilian mountain permafrost, Qinghai province, China. *Cold Regions Sci. Technol.* 66 (2-3), 93–104. doi:10.1016/j.coldregions.2011.01.008

Majorowicz, J. A., and Osadetz, K. G. (2001). Gas hydrate distribution and volume in Canada. *AAPG Bull.* 85 (7), 1211–1230. doi:10.1306/8626CA9B-173B-11D7-8645000102C1865D

Makogon, Y. F., Holditch, S. A., and Makogon, T. Y. (2007). Natural gas hydrates-A potential energy source for the 21st Century. *J. Petroleum Sci. Eng.* 56 (1-3), 14–31. doi:10.1016/j.petrol.2005.10.009

Makogon, Y. F. (2010). Natural gas hydrates - a promising source of energy. *J. Nat. Gas Sci. Eng.* 2 (1), 49–59. doi:10.1016/j.jngse.2009.12.004

Ning, F. L., Liang, J. Q., Wu, N. Y., Zhu, Y. H., Wu, S. G., Liu, C. L., et al. (2020). Reservoir characteristics of natural gas hydrates in China. *Nat. Gas. Ind.* 40 (8), 1–24.

Niu, Z. X., Geng, Q. M., and Dou, L. (2015). Palaeogeographic analysis of Muli coalfield Juhugeng coalmine area in Qinghai province. *Geol. Rev.* 61, 158–159.

Shakhova, N., Semiletov, I., Salyuk, A., Yusupov, V., Kosmach, D., and Gustafsson, O. (2010). Extensive methane venting to the atmosphere from sediments of the east siberian arctic shelf. *Science* 327 (5970), 1246–1250. doi:10.1126/science.1182221

Sun, Z. J., Yang, Z. B., Mei, H., Qin, A., Zhang, F., Zhou, Y., et al. (2014). Geochemical characteristics of the shallow soil above the Muli gas hydrate reservoir in the permafrost region of the Qilian Mountains, China. *J. Geochem. Explor.* 139, 160–169. doi:10.1016/j.gexplo.2013.10.006

Tan, F. R., Liu, S. M., Cui, W. X., Wan, Y. Q., Yang, C., Zhang, G. X., et al. (2017). Origin of gas hydrate in the Juhugeng mining area of Muli coalfield. *Acta Geol. Sin.* 91 (5), 1158–1167. doi:10.3969/j.issn.0001-5717.2017.05.015

Thomas, Z. A., Jones, R. T., Turney, C. S. M., Golledge, N., Fogwill, C., Bradshaw, C. J., et al. (2020). Tipping elements and amplified polar warming during the Last Interglacial. *Quat. Sci. Rev.* 233, 106222. doi:10.1016/j.quascirev.2020.106222

Wang, P. K., Huang, X., Pang, S. J., Zhu, Y., Lu, Z., Zhang, S., et al. (2015). Geochemical dynamics of the gas hydrate system in the qilian mountain permafrost, Qinghai, northwest China. *Mar. Petroleum Geol.* 59, 72–90. doi:10.1016/j.marpetgeo.2014.07.009

Wang, P. K., Zhu, Y. H., Lu, Z. Q., Bai, M., Huang, X., Pang, S., et al. (2019). Research progress of gas hydrates in the qilian mountain permafrost, Qinghai, northwest China: Review. *Sci. Sin. -Phys. Mech. Astron.* 49, 034606. doi:10.1360/sspma2018-00133

Wang, P. K., Zhu, Y. H., Lu, Z. Q., Huang, X., Pang, S., and Zhang, S. (2014). Gas hydrate stability zone migration occurred in the Qilian mountain permafrost, Qinghai, northwest China: Evidences from pyrite morphology and pyrite sulfur isotope. *Cold Regions Sci. Technol.* 98, 8–17. doi:10.1016/j.coldregions.2013.10.006

Wen, H. J., Shao, L. Y., Li, Y. H., Lu, J., Zhang, S. L., Wang, W. L., et al. (2011). Structure and stratigraphy of the Juhugeng coal district at Muli, Tianjun county, Qinghai province. *Geol. Bull. China* 30 (12), 1823–1828. doi:10.3969/j.issn.1671-2552.2011.12.003

Whiticar, M. J. (1999). Carbon and hydrogen isotope systematics of bacterial formation and oxidation of methane. *Chem. Geol.* 161 (1-3), 291–314. doi:10.1016/s0009-2541(99)00092-3

Ye, J. L., Qin, X. W., Xie, W. W., Lu, H. L., Ma, B. J., Qiu, H. J., et al. (2020). Main progress of the second gas hydrate trial production in the South China Sea. *China Geol.* 47, 557–568. doi:10.12029/gc20200301

Zhai, G. Y., Lu, Z. Q., Lu, H. L., Zhu, Y. H., Yu, C. Q., Chen, J. W., et al. (2014). Gas hydrate geological system in the Qilian Mountain permafrost. *J. Mineralogy Petrology* 34 (4), 79–92. doi:10.19719/j.cnki.1001-6872.2014.04.010

Zhang, F. G., Qin, A. H., Zhu, Y. H., Sun, Z. J., Zhang, S. Y., Wang, H. Y., et al. (2020). A discussion on geochemical migration mechanism of natural gas hydrate in Qilian Mountain permafrost. *Mineral. Deposits* 39 (2), 326–336.

Zhang, F. G., Tang, R. L., Zhou, Y. L., Zhang, S. Y., Sun, Z. J., and Wang, H. Y., (2019). An new tool for natural gas hydrate exploration-analysis of inert gas Helium Neon. *Acta Geol. Sin.* 93 (3), 751–761.

Zhao, X. M., Sun, Y. H., Deng, J., Rao, Z., Lu, C., Song, J., and Li, L. X., (2018). Microbial gas in the Mohe permafrost, Northeast China and its significance to gas hydrate accumulation in permafrost across China. *Acta Geol. Sin. Engl. Ed.* 92 (6), 2251–2266.

Zhou, Y. W., Guo, D. X., Qiu, G. Q., and Cheng, G. D., (2000). *China permafrost*. Beijing: Science Press, 1–450.

Zhu, Y. H., Lu, Z. Q., and Xie, X. L. (2011). Potential distribution of gas hydrate in the Qinghai-Tibetan Plateau. *Geol. Bull. China* 30 (12), 1918–1926. doi:10.3969/j.issn.1671-2552.2011.12.016

Zhu, Y. H., Zhang, Y. Q., Wen, H. J., Lu, Z., Jia, Z., Li, Y., et al. (2010). Gas hydrates in the Qilian mountain permafrost, Qinghai, northwest China. *Acta Geol. Sin. - Engl. Ed.* 84 (1), 1–10. doi:10.1111/j.1755-6724.2010.00164.x